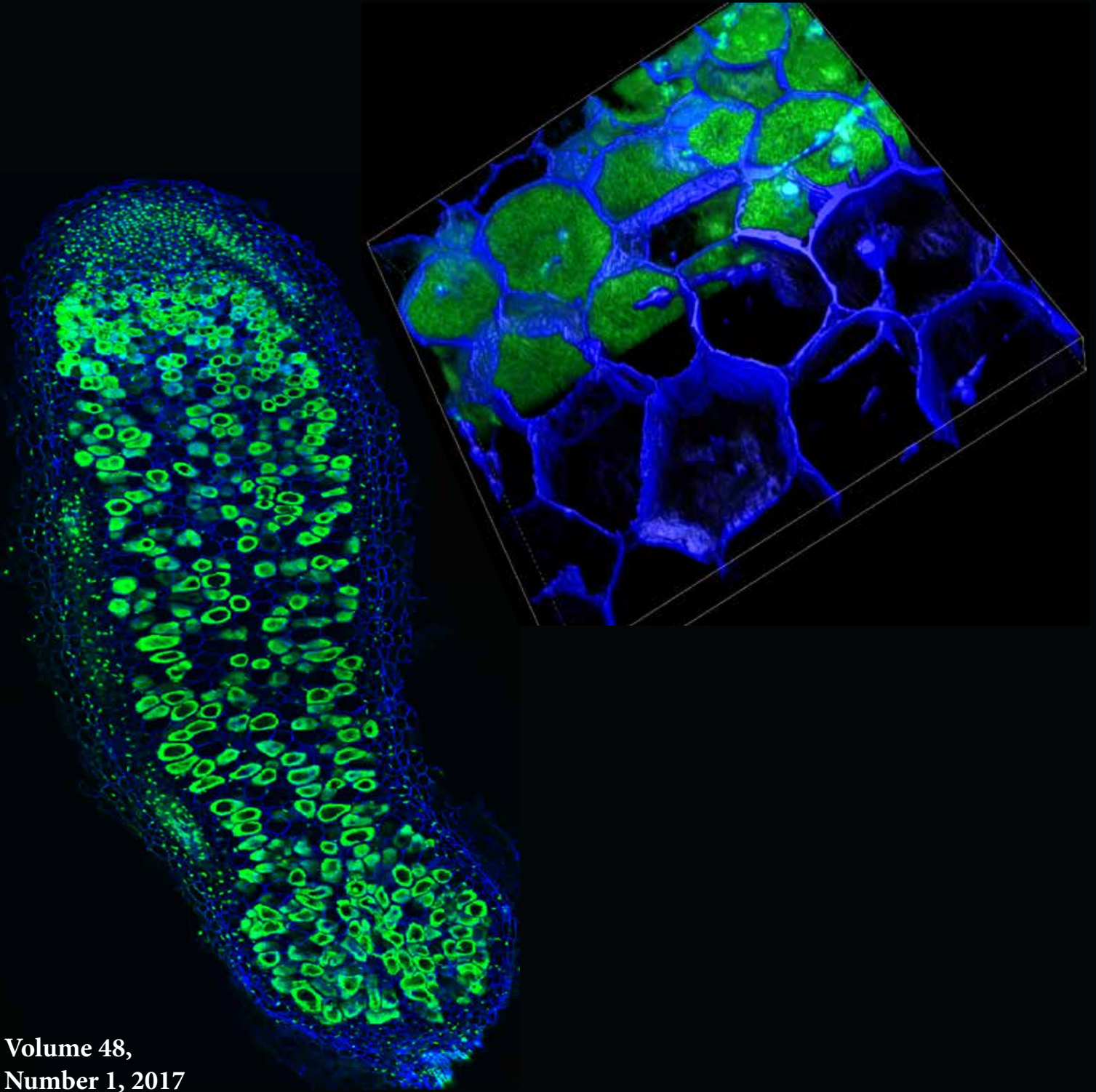


Texas Journal of Microscopy

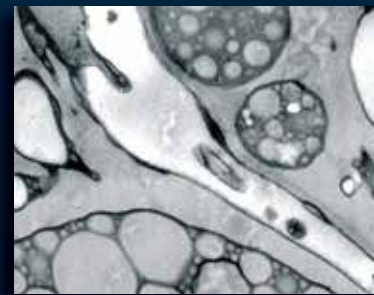
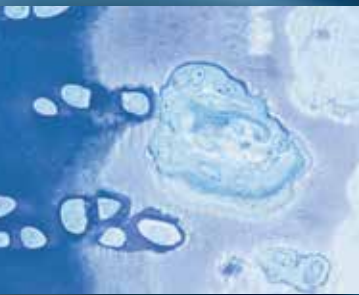


Volume 48,
Number 1, 2017
ISSN 1554-0820

Visit our website at www.texasmicroscopy.org

DiATOME *diamond knives*

**the highest quality...
the most precise sectioning...
incomparable durability**



building on 40 years of innovation

*ultra 45° • cryo • histo • ultra 35°
histo jumbo • STATIC LINE II • cryo immuno
ultra sonic • ultra AFM & cryo AFM*

NEW!... trimtool 20 and trimtool 45
*Finally, one trimming tool for all of your trimming
needs, be it at room or cryo temperatures.*

DiATOME U.S.

P.O. Box 550 • 1560 Industry Rd. • Hatfield, Pa 19440
Tel: (215) 412-8390 • Fax: (215) 412-8450
email: sgkcck@aol.com • stacie@ems-secure.com
www.emsdiasum.com

TSM OFFICERS 2016-2017

President

LAURA HANSON
Department of Biology
Texas Woman's University • Denton, Texas 76204-5799
(940) 898-2472 • FAX (940) 898-2354
lhanson@twu.edu

Past-President

SANDRA WESTMORELAND
Department of Biology
Texas Woman's University • Denton, Texas 76204-5799
(940) 898-2358 • FAX (940) 898-2354
swestmoreland@twu.edu

President-Elect

VACANT

Secretary

DAVID YAN
Characterization Center for Materials and Biology
University of Texas at Arlington, ELB 231
Arlington Texas 76019
(817) 272-0427 • FAX (817) 272-2358
davidy@uta.edu

Secretary-elect

VACANT

Treasurer

DAVID GARRETT
Dept. of Materials Science and Engineering
University of North Texas • Denton, Texas 76203-5017
(940) 369-8836 • dgarrett@unt.edu

Treasurer-elect

VACANT

Program Chairman

BERND ZECHMANN
Center for Microscopy and Imaging
Baylor University
One Bear Place #97046 • Waco, Texas 76798-7046
(254) 710-2322 • FAX (254) 710-2405
Bernd_Zechmann@baylor.edu

Program Chairman-elect

VACANT

APPOINTED OFFICERS

Corporate Member Representative

JAMES LONG
5794 W. Las Positas Blvd. • Pleasanton, CA 94588
(512) 657-0898 • jlong@gatan.com

Student Representative

VACANT

Journal Editors

CAMELIA MAIER
Department of Biology
Texas Woman's University • Denton, Texas 76204-5799
(940) 898-2358 • FAX (940) 898-2354 • cmaier@twu.edu

NABARUN GHOSH

Dept. of Life, Earth, and Environmental Sciences
West Texas A&M University • Canyon, Texas 79015
(806) 651-2571 • FAX (806) 651-2928
nghosh@mail.wtamu.edu

Webmaster

JIECHAO JIANG
Dept. of Materials Science and Engineering
University of Texas at Arlington • Arlington, Texas 76017
(817) 272-0841 • FAX (817) 272-2538 • jiang@uta.edu

Facebook Master

NABARUN GHOSH
Dept. of Life, Earth, and Environmental Sciences
West Texas A&M University • Canyon, Texas 79015
(806) 651-2571 • FAX (806) 651-2928
nghosh@mail.wtamu.edu

Contents



TEXAS JOURNAL OF MICROSCOPY VOLUME 48, NUMBER 1, 2017

ISSN 1554-0820

Editors

Camelia Maier, PhD
Department of Biology, Texas Woman's University, Denton, TX 76204

Nabarun Gosh, PhD

Dept. of Life, Earth, and Environmental Sciences, West Texas A&M University

Official Journal of the Texas Society for Microscopy

"TSM - Embracing all forms of Microscopy"

www.texasmicroscopy.org

President's Message	5
Spring 2017 Meeting Abstracts.....	6
Determination of Eggshell Thickness in FMG-Vaccinated Egg-laying Chickens, S.L. Westmoreland, E.D. Peebles and S.L. Branton	13
Corporate Members	20

Advertiser's Index:

Diatome	2
Gatan	4
Tousimis.....	19
Micro Star Technologies	23
Electron Microscopy Sciences	24

ON THE COVER

Confocal image of a *Medicago truncatula* (R108) root nodule harboring its symbiont, *Sinorhizobium meliloti* Sm1021 (left image). Rhizobia were stained with the nucleic acid stain Syto13 (green), and plant cell walls and infection thread walls were revealed by Calcofluor white staining (blue). The image on the upper right represents a 3-D reconstruction of a Z-stack. Infection threads, which serve as passageways for rhizobia, are seen entering and exiting host cells. Image by Dr. Catalina Pislariu, Texas A&M International University, Laredo, TX 78041-1900.

OneView Camera

10 nm

Gatan's award winning OneView camera sets the standard for imaging samples sensitive to beam damage or drift.

"My review would go something like this:

★★★★★ **Awesome camera**
Verified Purchase

This has been a great 4k camera for low-dose imaging. The low-dose imaging capabilities of the camera and the option for drift correction work great together! To be honest, I assumed the drift correction option would be something that I would never use. ... In reality, I have gotten **the best HRTEM** images from my samples using the drift correction option. ... This camera has given new life to my elderly TEM!

I would buy this camera again!

– Thomas M. Rea, Senior EM, 35 years

See how real-time drift correction allows you to record images before the sample stops drifting and guarantees the highest quality images at the lowest total dose, every time.

View our media library to learn more – www.gatan.com/MT-OV.



President's Message

It is an exciting time again for microscopists in Texas as we approach the 52nd annual meeting of the Texas Society for Microscopy. The meeting in Waco looks to be a stimulating event, organized extremely efficiently by Program Chairman Bernd Zechmann. Waco will be a new venue for most of us. On behalf of the Society I would like to thank Baylor University and the Waco Convention Center for hosting and the workshop sponsors, FEI and Leica. On Thursday there will be workshops on Focus Ion Beam Scanning Electron Microscopy with FEI and Automated Sample Preparation of Biological Specimens for TEM and SEM by Leica. Both workshops will be held in the state-of-the-art Center for Microscopy and Imaging at Baylor University. We are grateful to all of our corporate members and sponsors who do so much to support the Society. Bernd has also arranged a wonderful opportunity for socializing and networking with the social reception on Thursday evening at Ninfa's Mexican restaurant.

On Friday we can enjoy the meeting presentations, as well as anticipate outstanding presentations by the invited speakers. Dr. Debbie Kelly of Virginia Tech Carilion Research Institute will present on "Viewing dynamic biological systems in liquid at the nanoscale" as our life science speaker, while Dr. Ali Aliev of the Alan G. MacDiarmid NanoTech Institute of University of Texas at Dallas will be our Material Sciences speaker, talking about "Low-dimensional materials: structure, properties, and applications". Bernd has also organized an optional excursion on Saturday to experience downtown Waco, a marvelous opportunity to continue to interact with fellow microscopy enthusiasts and experts from across the state.

Last year's excellent meeting at Rice University in Houston, so ably organized by Emilie Ringe and Antony Stender, with Program Chairman Stephen Mick and Corporate Representative James Long is a hard act to follow, but Bernd

has risen to the occasion. In addition, I would like to thank all of the people who work so hard for TSM. David Garrett as our tireless Treasurer, David Yan as Secretary keeping everyone informed and records current, Past President Sandra Westmoreland for her support and continuing work for the Society, Jeichao Jiang as Webmaster, and Journal Editor Camelia Maier who continues to design and produce an outstanding Texas Journal of Microscopy with the able assistance of Facebook designer and Journal Co-Editor Nabarun Ghosh.

As happens with many societies, membership and attendance rises and falls over time. I encourage the membership to serve as ambassadors for the Society and help make colleagues aware of the opportunities both for students and more established scientists to present at our meetings and serve the Society. I am fairly new to the TSM, having previously served as Life Science Program Chair, but have already seen how beneficial the opportunities can be, especially for students. As we continue into our 53rd year, I hope to see the TSM continue to thrive and grow.

It has been an honor to serve as President during the past year.

Laura Hanson
TSM President, 2016-2017



Abstracts

BIOLOGICAL SCIENCES Spring 2017

ROLE OF WALL TEICHOIC ACID IN THE NET CHARGE OF *STAPHYLOCOCCUS AUREUS* CELL WALL AND ITS IMPORTANCE IN BIOFILM FORMATION. BINAYAK RIMAL*, CHENGYIN LIU[§], JAMES CHANG[§], and SUNG JOON KIM[§], Biomedical Studies Institute* and Chemistry and Biochemistry[§] Department, Baylor University, Waco Texas

Biofilm is a colony of sessile and dormant bacteria surrounded by extracellular matrix that enhances its ability to survive through inimical environment. *Staphylococcus aureus* is the leading Gram-positive pathogen for biofilm-related nosocomial infections such as those arising from biofilm on indwelling catheters, endocarditis on prosthetic cardiac valves, and septic arthritis on joint replacements. Biofilm serves as a reservoir of pathogens for persistent infection with the translocation of bacteria from the primary to secondary sites of infection. While the exact composition of *S. aureus* biofilm is unknown, it is widely thought that the biofilm matrix consists of wall teichoic acid (WTA), peptidoglycan, poly-N-acetylglucosamine, extracellular DNA, and proteins. Interactions between these components are thought to be crucial for the initiation of cell-cell aggregation, biofilm growth, maturation, and disassembly. In this study, we characterized the biofilm formation and disassembly of SA113, a prolific biofilm forming *S. aureus* strain, using focused ion beam scanning electron microscopy (FIB-SEM) in conjunction with electron dispersive x-ray spectroscopy (EDS). EDS analysis was performed on SA113 biofilm at 20KV using an Octane Pro Silicon Drift Detector (EDAX, Mahawah, NJ, USA), spot size 7, and at a working distance of 10mm. We found that excess sodium ions were bound to the biofilm matrix, with approximately 2.7-fold increase from the atomic abundance observed for the planktonic bacteria. EDS analysis of isogenic Δ tagO deletion mutant, which does not form biofilm and lacks WTA, showed the absence of sodium ion binding. This indicated that the biofilm matrix is a) highly negative charged and b) the negatively charged phosphate backbone in WTA plays an essential role in the assembly of biofilm.

EFFECTS OF ESTRADIOL AND BRASSINOLIDE ON GROWTH AND REPRODUCTION OF *ARABIDOPSIS THALIANA*. LAUREN HILZ and CAMELIA MAIER, Texas Woman's University, Department of Biology, Denton, Texas, 75201

Estradiol (ES) is a steroid hormone that has important functions in the reproduction and development of vertebrates but little is known about its effects on plants. Brassinolide (BS) is the only known plant steroidal hormone with essential roles in the regulation of multiple physiological and developmental processes. The objective of this study was to compare the effects of ES and BS on the germination, growth and reproduction of *Arabidopsis thaliana*. Seeds of *A. thaliana* Columbia (col-1) were soaked in 10 nM ES, 10 nM BS and 0.01% ethanol (solvent for hormones, used as a control group) overnight and then shown in pots with pre-sterilized soil. Seeds with no treatment were also used as a second control group. Plants were grown in a growth chamber under 16-hour light, 23°C, 60% relative humidity. Every week the seedlings were sprayed with the hormone solutions for a total of three weeks. Cotyledons and leaves were collected over 21 days and analyzed with a Hitachi T1000 SEM for changes in number of stomata and density of epidermal cells and trichomes. Growth and reproductive data, such as number of inflorescences and flowers, were collected on day 28. This study also provided an opportunity for testing the Talbot and White's (2013) methanol fixation of plant tissue for SEM since it was advertised as a technique that improves preservation of tissue morphology and especially cell dimensions. Results show the highest increase in cell size, number of inflorescences and flowers in plants under BS treatment followed by plants treated with ES in comparison with ethanol and no treatment control groups. The methanol fixation method introduced by Talbot and White was not as effective with our plants as they observed in their study. *Arabidopsis* plant tissue was dried out and wrinkled creating difficulties in measuring cells. In conclusion, both BS, a plant steroidal hormone, and ES, an exogenous steroidal hormone, have a beneficial effect on plant growth and development. Since the treatment effects were similar, ES may have the same mechanism of action as BS. Additional research is needed to determine the mechanism of action of ES on plants. This project also helps us understand how mammalian sex hormones in the environment effect plant growth.

MICROTECHNIQUES FOR FUNCTIONAL GENOMICS OF SYMBIOTIC NITROGEN FIXATION

*CATALINA PISLARIU^{1,2}, MARIE BOURCY³, JIN NAKASHIMA¹, PASCAL RATET³, MICHAEL UDVARDI¹

¹The Samuel Roberts Noble Foundation, Plant Biology, Ardmore, OK, USA;

²Texas A&M International University, Laredo, TX; ³ISV-CNRS, Gif Sur Yvette, France

Leguminous plants can thrive in less fertile soils because of their ability to establish symbiotic associations with nitrogen-fixing soil bacteria, collectively known as rhizobia. To gain insight into the genetic and molecular mechanisms governing this symbiosis, several resources have been developed for functional genomics in the model legume *Medicago truncatula*, including the genome sequence, the Gene Expression Atlas (MtGEA), and tobacco retrotransposon *Tnt1*-insertion and fast neutron bombardment (FNB) deletion mutant populations. SNF involves the development of new organs, root nodules, a complex process requiring coordinated regulation of thousands of plant and bacterial genes. Only a fraction of these genes has been characterized functionally. Uncovering new genetic controls of infection and nitrogen fixation efficiency has the potential to inform low input agricultural practices. *Tnt1*-tagging introduces multiple insertions into the plant genome for saturation mutagenesis. From a *Tnt1*-insertion mutant population of *M. truncatula*, we isolated 179 mutants impaired in nodule development and SNF during symbiosis with *Sinorhizobium meliloti* (Pislariu *et al.*, 2012). Only 39 mutants are insertion alleles of known symbiotic genes, thus, many more genes remain to be discovered.

Histological techniques and observations using bright-field, confocal, and transmission electron microscopy were used to identify defects at organ and cellular level in several potentially new symbiotic mutants, including one that lacks the activity of a PLAT (Polycystin-1; Lipoxygenase, Alpha-Toxin) domain gene (*MtNPD1*), and one defective in a putative phosphatidylinositol phospholipase C-like protein (*DNF2*). Although early stages of nodule development and bacterial colonization appeared to be normal in *npd1*, nodules ceased to grow, remaining small and round (Fig. 1 B). In contrast, *dnf2* nodules elongate almost to the extent of wild-type, but display symptoms of early senescence. Microscopic observations revealed that rhizobia colonizing *npd1* nodules appeared to decay prematurely, as suggested by reduced nodule occupancy (Fig. 1 B), lower fluorescence intensity and cellular disorganization (Fig. 1 D), and by loss of symbiosome (rhizobia encased into a plant-derived membrane) content (Fig. 1 F). Live-dead staining with Syto9 and Propidium Iodide was also used in *npd1* and

dnf2 to demonstrate that the symbiosome membranes were compromised in both mutants. Using a combination of microscopic and molecular techniques, we found that both *MtNPD1* and *DNF2* are critical for accommodation of rhizobia inside host cells, and prevent early nodule senescence.

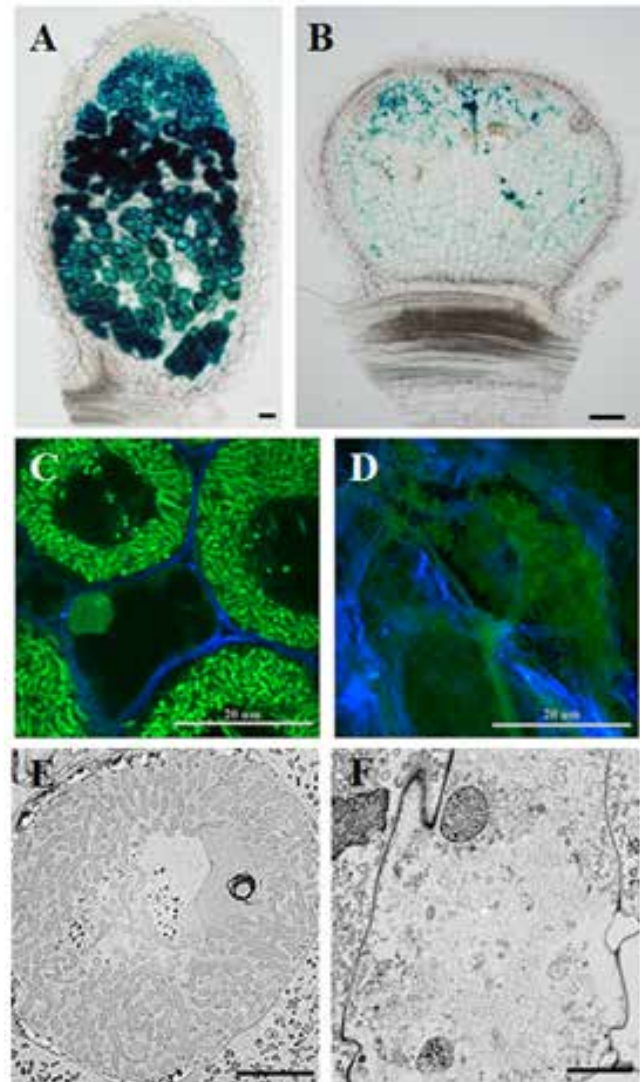


Fig. 1 – Symbiotic phenotype of wild-type (A, C, E) and *npd1* (B, D, F) nodules imaged by bright-field (A, B), confocal (C, D), and transmission electron (E, F) microscopy. *Npd1* nodules lack a functional PLAT domain gene. In panels A and B, *S. meliloti* express a *hemA::LacZ* gene. In panels C and D, rhizobia were stained with Syto13. Scale bars: 50 μ m (A, B), 20 μ m (C, D), and 10 μ m (E, F).

CHARACTERIZATION OF TWO- AND THREE-DIMENSIONAL ULTRASTRUCTURAL CHANGES INDUCED BY ZUCCHINI YELLOW MOSAIC VIRUS IN PUMPKIN PLANTS

BERND ZECHMANN

Baylor University, Center for Microscopy and Imaging, One Bear Place #97046, Waco, TX 76798-7046, USA

Zucchini Yellow Mosaic Virus (ZYMV) belongs to the genera of Potyvirus and induces severe symptoms on plants such as stunting, yellowing, and deformation of the leaves and fruits. At later stages of infection, leaves develop a yellow mosaic and often form dark green blisters (Fig. 1A). The aim of this study was to investigate two- and three-dimensional (3D) ultrastructural changes induced by ZYMV in *Cucurbita pepo* L. by using TEM and to correlate these changes with the spread of ZYMV throughout the plant. Negative staining revealed that, after inoculation of the cotyledons, ZYMV-particles could be found as long, flexuous, rod-shaped structures (707nm x 12 nm) in the sap of roots 3 days post inoculation (dpi). They were then

detected in the apical meristem 5 dpi, and could finally be found throughout all plant parts 9 dpi. These results demonstrate that after inoculation ZYMV moved from the cotyledons into the roots first before it travelled upwards through the stem to systemically infect the whole plant. Within the cytosol of root, stem and leaf cells, ZYMV induced the formation of cylindrical inclusions (CI) (Fig. 1B). On a 3D level, these structures formed long tubular scroll like structures which had a preferred orientation throughout the cytosol and showed an average length and width of 3 μ m and 120 nm, respectively. As CIs were often found to be correlated with plasmodesmata they are most probably involved in cell to cell movement of the virus.

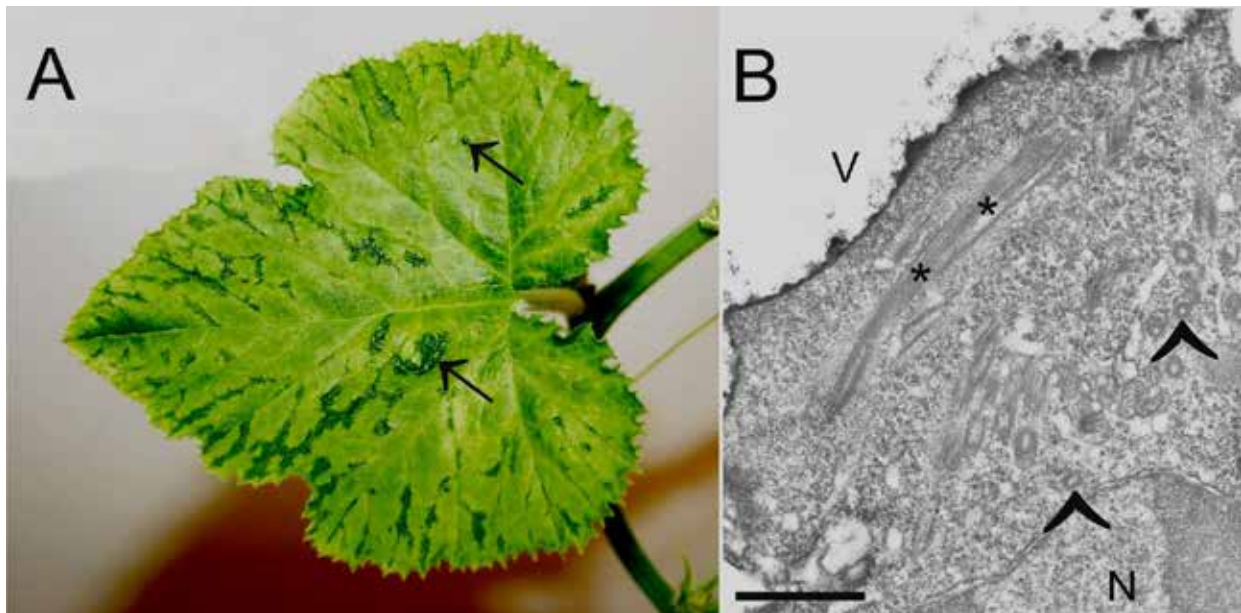


Figure 1. Leaf of ZYMV-infected plant (A) showing strong symptoms such as yellowing and dark green blisters (arrows). ZYMV-infected plant cell (B) showing cylindrical inclusions in the cytosol as scroll like structures (arrowheads) and bundles of filaments (stars). N = nucleus, V = vacuole. Bar = 1 μ m.

TESTOSTERONE MAINTAINS SPERMATOGENESIS BY PREVENTING GERM CELL APOPTOSIS: IS TESTOSTERONE ACTING DIRECTLY ON GERM CELL MEMBRANE PROGESTERONE RECEPTORS?

ARPITA TALAPATRA¹, SHUVALAXMI DASGUPTA¹, DIBYENDU DUTTA², NATHANIEL MILLS¹,¹Department of Biology, Texas Woman's University, Denton, Texas, ²Department of Professional Sciences, Middle Tennessee State University, Murfreesboro, Tennessee

Ethylene dimethane sulfonate ablates Leydig cells and depletes serum testosterone to undetectable levels. Germ cells, lost by apoptosis, were found in rat testicular tissue harvested at 7 and 10 days post-EDS. Regression of germinal epithelium was time dependent and correlated with decreased testicular weight. Apoptotic cells were identified by TUNEL staining. Changes in gene expression were measured using reverse transcription qPCR. Significant differences of *Bcl2* genes at 7 and 10 days were observed when compared to vehicle controls. The levels of Fas and FasL increased while caspases exhibited variable levels. Germ cell detachment from Sertoli cells that exhibited cytoskeletal disorganization was also observed. Immunostaining indicated that androgen receptors were found in Sertoli cell nuclei, and myoid cell nuclei of the seminiferous tubule. Some staining was observed in the stripped cytoplasm of spermatids, although androgen receptors have not been reported in germ cells. Testosterone receptor (AR, NR3C4) and progesterone receptor (PR, NR3C3) are structurally similar and testosterone at double the progesterone concentration will compete with progesterone for progesterone receptor activation. We have initiated studies to find and characterize mRNAs for mPRs and membrane progesterone/adiponectin receptors (mPAQRs) by RT – qrtPCR. At least 5 mPRs mRNAs [*Paqr(s)*] expressed in testes were identified using total RNA from whole testes. The cells of origin for these mRNAs are not known. Germ cell suspensions will be stained with fluorescently labeled testosterone and progesterone to identify an alternate pathway (mPRs) of testosterone action that may show germ cells to be a direct target of testosterone. *Supported by Texas Woman's University Research Enhancement Program 2016.*

ANALYZING THE ROLE OF THE HUMAN MCM8 AND MCM9 DOMAINS IN MITOMYCIN C INDUCED STRESS.

SHIVASANKARI GOMATHINAYAGAM^a, ELIZABETH C. JEFFRIES^b, MICHELLE A. WOOD-TRAGESER^c, SVETLANA YATSENKO^c, ALEKSANDAR RAJKOVIC^c, MICHAEL A. TRAKSELIS^a,^aDepartment of Chemistry and Biochemistry, Baylor University, ^bDepartment of Chemistry, University of Pittsburgh, ^cDepartment of Obstetrics, Gynecology, and Reproductive

Sciences, Magee-Womens Research Institute, University of Pittsburgh.

MCM8 and MCM9 helicases are newly identified members of the MCM (minichromosome maintenance) family and contain conserved DNA binding and AAA+ helicase domains. The MCM8 and MCM9 helicases participate in resection of DNA double strand breaks (DSBs) through homologous recombination (HR) and in meiotic recombination. Familial mutations in either MCM8 or MCM9 are causative agents for infertility, premature ovarian failure (POI), and chromosome instabilities in patients. Identified genetic changes include nonsynonymous SNPs, nonsense mutations, and splice site mutations. In all cases, either MCM8 or MCM9 has impaired function leading to POI and genomic instabilities. The mutated phenotypes are consistent with the inability to resolve crossover intermediates required for mitotic or meiotic recombination. Immunofluorescence imaging was performed in MMC treated HEK-293T cells transfected with GFP tagged wild type or mutant (MCM8 P149R and MCM9 1732+2T>C or BRCv-MCM9) protein. Using immunofluorescence microscopy, we have identified that patient mutations when replicated in the cells inhibit the formation of MCM8/9 repair foci upon MMC treatment. We have also identified a new BRCv domain in MCM9 that is also shown to be required for the formation of MMC-induced MCM9 repair foci. Our work suggests that MCM8 and MCM9 are required for the repair of MMC-induced DNA lesions through homologous recombination and to maintain genomic stability.

MICROSCOPIC ANALYSIS TO ASSESS THE REDUCTION OF INDOOR PARTICULATE MATTER, AEROLLERGEN AND ANIMAL DANDER USING AHPCO® AND PLASMA HYBRID NANOTECHNOLOGY.

NABARUN GHOSH¹, CHANDINI REVANNA², AUBREY HOWARD¹ NELOFAR SHERALI¹, JON BENNERT³, JEFF BENNERT³ and CONSTANTINE SAADEH⁴, ¹Department of Life, Earth and Environmental Sciences, West Texas A&M University, Canyon, Texas 79015, ²Department of Environmental Health & Safety, Texas Tech University, Lubbock, TX 79409, ³Air Oasis, Amarillo, Texas 79118, ⁴Allergy ARTS, Amarillo, Texas 79124.

The allergy and asthma cases have doubled since 2007 (Angling and Ghosh, 2014). Analysis of 17-years aeroallergen data of the Texas Panhandle using a Burkard Spore Trap showed a steady increase in aeroallergen counts (Ghosh *et al.*, 2016). We evaluated the newly developed air purifier that uses both the Bi-Polar® and AHPCO. The AHPCO and Bi-Polar nanotechnologies are used in air

purification, contaminant-free ice production in restaurants and hospitals. A hybrid AHPCO or Advanced Hydrated Photocatalytic Oxidation and Plasma Nanotechnology were implemented in the new generation Air Oasis air purifiers. This purifiers use AHPCO technology, which produces a blanket of redundant oxidizers that not only clean the surrounding air, but target the particulate matters in the air as well as on the surfaces and thus sanitize the air. The Bi-Polar® creates cold plasma discharge which consists of positive and negative ions from water vapor in the air. Positive and negative ions attach to particles and allergens such as dust, smoke, pollen and dander. Particles cluster together to create larger and heavier particles, which drop out of the air. We compared the aeroallergen, dander and overall particle count in two fiber glass chambers by exposing the glass slides with double sticky tape at varied times between 24-120 hours. Particle counts were recorded to assess the capacity of sterilization. In the fiberglass chambers we used a Dylos Air Quality Monitor to detect and compare the particle counts with and without (control) running the air purifier for 24, 48, 72 and 120 hours. The slides with the collected samples were observed with a BX-40 Olympus digital microscope. The data from the captured images were analyzed using Image Pro 6.0 Plus software. A significant reduction in the total particle count, including various aeroallergens and animal dander, was found when the air purifiers were used.

MATERIALS SCIENCE Spring 2017

LOW-DIMENSIONAL MATERIALS: STRUCTURES, PROPERTIES and APPLICATIONS. ALI ALIEV, University of Texas at Dallas, Alan G. MacDiarmid NanoTech Institute, Richardson, TX 75080

Low dimensional materials refer to those systems in which at least one of the three dimensions is intermediate between the characteristic of atoms/molecules and those of the bulk material, generally in the range from 1 nm to 100 nm. Examples of low dimensional materials are 2-dimensional graphene, 1-dimensional carbon nanotubes and 0-dimensional quantum dots. In these materials the cross-section in reduced direction is lower than de-Broglie wavelength of electrons. The dimensional constraint on the system gives rise to quantum size effects, which can significantly change the energy spectrum of electrons, phonons and other quasiparticles. As a result, some properties of such systems are very different from those of their bulk counterparts. These materials have shown a wide range of intriguing phenomena and extraordinary

electronic, optical, thermal, mechanical and chemical properties, which result in huge interest for their application in nanotechnology, biology and medicine. This presentation will focus on the applications of low-dimensional materials developed in our laboratories and worldwide.

GRAPHENE / MULTI-WALLED CARBON NANOTUBES IN THIN FILM SPONGE FOR THERMOACOUSTIC PROJECTORS. JAMES PENNEY*, ALI ALIEV, and Alan G. MacDiarmid NanoTech Institute, Richardson, TX 75080, The University of Texas at Dallas, Richardson, Texas 75080

Graphene/Multi-Walled Carbon Nanotubes (MWCNT) are nanomaterials that have high potential for thermal applications. Our goal is to create thin film sponges of Graphene/MWCNT to be used as thermoacoustic (TA) projectors. The plan is to make mechanically and chemically stable conductive film competing with free-standing carbon nanotube sheets. MWCNT add mechanical stability to the thin film sponge. The solution for the thin film sponge was made from a combination of two suspensions, MWCNT and Graphene Oxide (GO). MWCNT were dispersed in water with Triton X-100 surfactant and GO was dispersed in water at 4 mg/mL. The solutions were combined at a ratio of four parts GO suspension and 1 part MWCNT suspension. The obtained final solution was sonicated for forty-five minutes at 60% maximum power. The dispersed solution was place on an aluminum dish to be frozen and dried. The remaining material was a thin film sponge roughly 1 mm in height. While the MWCNT help with mechanical stability, the suspension also helps making the solution less hydrophobic, which allows for thinner film. The sponge was then annealed in an argon furnace at 700° C for thirty minutes to reduce oxygen in the material and increase conductivity. Thermoacoustic testing with a wide range of frequencies was performed on the annealed sponge. We have been able to create a thin film sponge that has demonstrated high TA projector performance. Characterization of this annealed sponge was performed with SEM (Fig. 1).

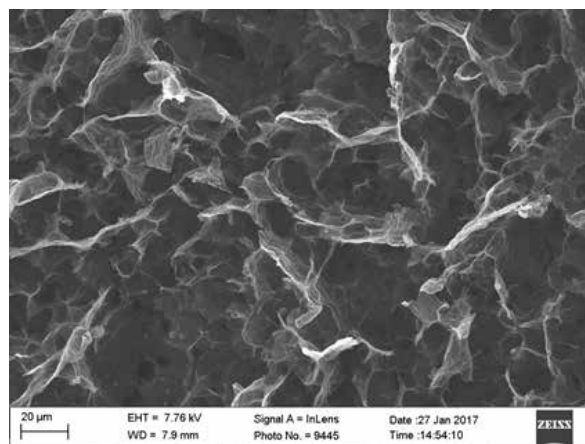


Fig. 1 – Graphene/MWCNT thin film sponge after annealing

TECHNICAL ABSTRACTS

Spring 2017

DEVELOPMENT AND OPTIMIZATION OF AN ULTRA-HIGH SPATIAL/MASS RESOLUTION CHEMICAL MICROSCOPE WITH FIB-SEM CAPABILITIES

RAUL A. VILLACOB, MATTHEW R. BRANTLEY, IAN ANTHONY, TOURADJ SOLOUKI

Department of Chemistry, Baylor University, Waco, Texas 76706

Mass spectrometry imaging (MSI) based chemical microscopy has been a growing area of interest in the material and biomedical sciences and has enabled researchers to interrogate complex cellular processes. Previously, ion projectiles [e.g., focused ion beam (FIBs)] have been coupled with high resolution mass spectrometry (MS) to create powerful Fourier Transform Ion Cyclotron Resonance-Secondary Ion Mass Spectrometers (FT-ICR-SIMS). However, insufficient sputtered ion yields have limited the useful lateral resolution to several hundred microns (1). Secondary Neutral Mass Spectrometry (SNMS) research have shown that having localized electron clouds increases sputtered ion yields at the local area of primary ion impact (2). Few reports exist in the literature for FT-ICR microscopy instrumentation and thus extensive testing and optimization is required to produce a nanoscale-resolution-capable FT-ICR SIMS.

In this presentation, we will show results from optimization of a custom designed imaging mass spectrometer. This novel MS is equipped with state-of-the-art components with the goal of achieving ultra-high mass resolution and sensitivity (via an FT-ICR mass analyzer), extreme spatial resolutions and reproducibility (via a liquid gallium FIB and custom-engineered sample stage), and electron-based modular post-ionization. In addition, the theoretical optimization of the charged particle/ion optics of the aforementioned instrument will be discussed. The imaging MS outlined in this presentation was designed with several features in mind, all of which emphasize a modular and expandable architecture. A liquid-gallium FIB is designed to be housed above the sample stage. The incident angle of the FIB beam (with respect to the sample plane) can be adjusted by motorized rotation of the custom sample stage. Rough sample positioning (>100 nm precision in a 41x26x26 mm volume) and incident angle optimization (>500 μ° precision) can be achieved. During optimization, the sample can be imaged using focused ion beam-secondary electron microscopy (FIB-SEM) in a beam-raster configuration. During MS analysis, rastering is achieved using the final 2 axes of nano-positioners, which are attached to the rotational axis (>1 nm resolution in a

38x38 μm area). Rastering the stage, as opposed to the beam, provides improved spatial precision and reproducibility. Vacuum chambers were repurposed from older FT-ICRs (formerly IonSpec now Agilent Technologies, CA) or manufactured housings (Kurt J. Lesker Company, PA; MDC Vacuum Products LLC, CA). A liquid-gallium FIB and CDEM detector system (BDS-50/BDS-200, FEI Company, OR/ Frencken America, Inc.) is used to focus ions on a custom integrated 6-axis sample stage (SmarAct Inc, CA; Piezosystem Jena, Inc., MA). System control utilizes custom LabVIEW software (National Instrument, TX) and PXIe hardware. Data is performed utilizing our custom-analysis platform "DataShop". Bias voltages and waveforms can be generated by a custom MIPS system (GAA Custom Engineering, WA, USA).

SIMION 8.1 (SIS, NJ, USA) theoretical ion trajectory calculations were employed in conjunction with SolidWorks computer-assisted design (CAD) software (Dassault Systemes, France). To maximize simulation performance, individual geometry files were created as hand-coded .gem files for each of the instrument segments (e.g. extraction assembly, transfer quadrupole, ICR cell, etc.) and collated into a single workbench. A Monte-Carlo approach, implemented in Python and MatLab (MathWorks, MA, USA), was developed to optimize key instrument parameters (e.g. lens voltages, RF potentials, trapping times, etc.) and report ion transmission at various stages in a unified format. Initial theoretical optimizations were performed manually using heuristically determined starting voltages/frequencies. Optimized ion transmission into the FT-ICR was measured at 40% (out of 1000 ions per run). Because radio-frequency ionization (RFI) has never been utilized for post-ionization, as we have utilized for our system, further study was required for optimizing geometry and interrogating the effect on ion trajectories. After initial proof of concept validation of the ion optics, an automated Monte-Carlo approach was devised for the optimization of the ion optics, as well as the post-processing of the trajectory data. Using a custom-developed Python script, potentials and RF frequencies were randomized within pre-determined bounds for each electrode and submitted

to separate SIMION simulations (1 for each available CPU core). Results were tabulated into CSVs that were submitted to a custom MATLAB program (The MathWorks, CA, USA). Summary of our findings from SIMION calculations and ion transfer/detect optimization will be presented.

Acknowledgments: The authors would like to acknowledge the financial support provided by the National Science Foundation (NSF), (NSF-IDBR Award # 1455668).

References

1. Smith, D.; Kiss, A.; Leach, F.; Robinson, E.; Paša-Tolić, L.; Heeren, R. *Analytical and Bioanalytical Chemistry* 2013, 405, 6069-6076.
2. Müller, U.; Schittenhelm, M.; Schmittgens, R.; Helm, H. *Surface and Interface Analysis* 1999, 27, 904-910.

VIEWING DYNAMIC BIOLOGICAL SYSTEMS IN LIQUID AT THE NANOSCALE

DEBORAH F. KELLY

Virginia Tech Carilion Research Institute and Department of Biological Sciences, Virginia Tech, Roanoke, VA 24016

Understanding the properties of molecular machines is a common goal of biologists and engineers. Technical barriers in high-resolution imaging can limit our knowledge of dynamic events at the nanoscale level. Transmission electron microscopy (TEM) permits us to peer into the world of cells and molecules. However, functional machines must be fixed in order to enter the ultrahigh vacuum system of a TEM. This task is typically accomplished by freezing specimens at high velocity in a thin layer of vitreous ice. Although ice preserves the structural features of biological assemblies, it also arrests them, making it difficult to understand dynamic mechanisms. Recent advances in the development of materials, such as graphene and silicon nitride, provide new opportunities for TEM imaging in real-time. Here we demonstrate our efforts to exploit these new materials and to create environmental chambers that permit us to perform experiments *in situ* or “inside” the TEM column using microfluidic technology. Using the Poseidon specimen holder (Protochips, Inc.), we can now view biological machinery in a native liquid environment with nanometer resolution (Fig. 1). This new imaging modality allows us to visualize dynamic mechanisms in a completely new way. We are currently employing Liquid Cell-TEM to improve our view of molecular events involving viral and cellular processes for biomedical applications.

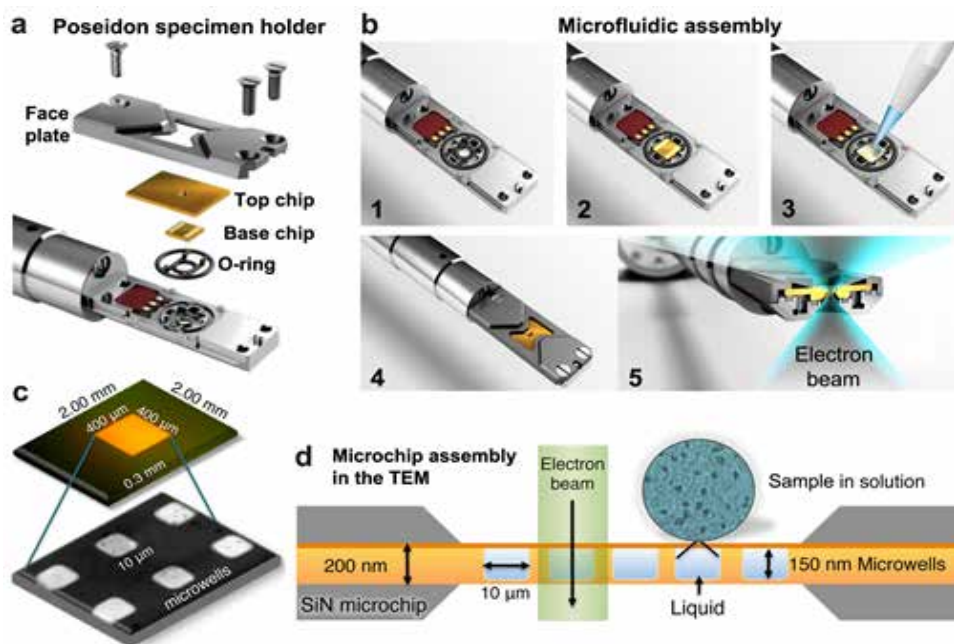


Fig. 1 – The Poseidon Select system for LC-TEM. (a) The Poseidon Select microfluidic specimen chamber. (b) The base chip of the assembly is placed on top of an O-ring fitting (1-2), while the liquid specimen is added to the base chip (3). The top chip is then hermetically sealed (4) prior to placing in the TEM column (5). (c) The base chip encompasses microwells, transparent to the electron beam. (d) Cross-section through the specimen assembly accommodates a 150-nm solution sample. (Adapted from DiMemmo *et al.*, *Lab Chip*, 2017).

DETERMINATION OF EGG SHELL THICKNESS IN FMG-VACCINATED EGG-LAYING CHICKENS

SANDRA L. WESTMORELAND¹, E. DAVID PEEBLES², AND SCOTT L. BRANTON³

¹Texas Woman's University, Department of Biology, Denton, Texas 76204

²Mississippi State University, Department of Poultry Science, Mississippi State, Mississippi 39762

³USDA-ARS, Poultry Research Unit, Mississippi State, Mississippi 39762

Abstract

Mycoplasma gallisepticum (MG) is a pathogen that causes chronic respiratory disease in chickens. MG is easily transmitted from bird to bird and there is no cure. F-strain *Mycoplasma gallisepticum* (FMG) is approved by the United States Department of Agriculture (USDA) for use as a live attenuated vaccine to protect commercial layer chickens against wild strain MG infections. The purpose of this study was to investigate the effects on eggshell thickness in eggs laid by FMG-inoculated Single Comb White Leghorn pullets of Hy-Line variety W-36. Other variables in the experiment included three diets (basal diet; 2% poultry fat added; and 2% poultry fat plus phytase and 25-hydroxycholecalciferol added) and two ages of lay (24 weeks and 50 weeks). Two replicate trials were performed. Eggshell cross section samples for each combination of variables (control versus experimental, diet, and age of lay) were imaged and measured using scanning electron microscopy and digital image analysis. It was determined that there were no significant main or interaction effects for either trial. We conclude that, although the factors in this investigation (inoculation with FMG, diet, and age of lay) may affect the reproductive tract in some ways, our study shows that these effects were not manifest in the thickness of the shells that were examined. This study demonstrates the use of an innovative method for eggshell thickness measurement using SEM and image analysis.

Key Words: *Mycoplasma gallisepticum*; vaccine; avian eggshell, SEM

List of Abbreviations: FMG - F-strain *Mycoplasma gallisepticum*; MG - *Mycoplasma gallisepticum*; PF - poultry fat; 25-D3 - 25-hydroxycholecalciferol.

Introduction

Mycoplasma gallisepticum (MG) is a pathogen that causes chronic respiratory diseases in chickens. The infection is easily transmitted bird-to-bird and, once infected, a bird is infected for life. The disease results in great economic loss worldwide. It causes decreased egg production, loss in body weight and hatchability, reduced feed conversion, and increased medical costs (Burnham, *et al.* 2002, Vance, *et al.* 2009). MG is a mycoplasma, which is a minute prokaryotic organism (125-250 micrometers) that has a simple ultrastructure including a cell membrane, ribosomes, and a nucleoid region, but no cell wall. Due to the lack of a cell wall, mycoplasmas are resistant to antibiotics that interfere with cell wall synthesis and they are not susceptible to lysis by detergents and alcohols (Khan, *et al.* 1986). These properties of mycoplasmas have led to the development of vaccines to help prevent MG infection in commercial flocks.

Vaccination of layers with live MG is commercially available to protect flocks against natural infections. Live attenuated MG vaccines for table egg chickens were initially

approved by the United States Department of Agriculture (USDA) in 1989 to help control MG outbreaks. One MG vaccine, F-strain *Mycoplasma gallisepticum* (FMG), has been shown to protect flocks from field strains of MG (Peebles, *et al.* 2003).

Numerous research studies have been conducted to investigate possible side effects of the FMG vaccine on laying hens and their eggs. Factors which have been investigated include: FMG vaccination effects on structure of the birds' digestive and reproductive organs; effects of inoculation date on egg production; effects on hen mortality and body weight; and effects on hens' blood characteristics including whole blood hematocrit, plasma protein, serum cholesterol, triglycerides, and calcium (Burnham *et al.* 2002a, Burnham *et al.* 2002b, Burnham *et al.* 2003). In addition, attention has been given to the characteristics of eggs produced by vaccinated birds including studies on egg production, egg quality, egg weight, and eggshell breakage and strength (Burnham *et al.* 2002, Burnham *et al.* 2003, Peebles *et al.*

2003a, Peebles *et al.* 2003b, Vance *et al.* 2008).

In an attempt to ameliorate potential effects of the FMG vaccine, such as decreased egg production, decreased egg weight, and changes in internal egg and eggshell characteristics, researchers have investigated the use of dietary supplements including poultry fat (PF), phytase, and 25-hydroxycholecalciferol (25-D3). Peebles *et al.* (2003) suggested that the addition of supplemental dietary fat (1.5% PF) may provide lipids necessary for the maintenance of egg yolk formation and subsequent egg production in infected birds, which may help prevent reductions in egg production due to FMG in laying hens. However, a study by Peebles, *et al.* (2008) determined that FMG-inoculated birds whose diet was supplemented with phytase and 25-D3 had no effect on total egg production, egg weight, or any of the internal egg and eggshell characteristics. The eggshell thickness was not measured in this experiment. Instead, eggshell was measured by means of eggshell weight per unit of surface area (Peebles *et al.*, 2008).

Materials and Methods

Experimental Setting

The purpose of this study was to determine the effect of vaccination of commercial layers with FMG on eggshell thickness. Research questions that were addressed in this study were as follows: 1. What are the effects of FMG vaccine on eggshell thickness?; 2. Does shell thickness of inoculated birds vary with age?; and 3. Does diet alter the effects of FMG inoculation?

The experiment involved multiple variables in addition to the vaccination, including three different diets (basal diet: 2% PF added; and 2% PF plus phytase and 25-D3 added) and two ages of lay (24 and 50 weeks). Cross section micrographs were taken on each eggshell using scanning electron microscopy and thickness measurements were made using image analysis software. A time replicate of the experiment was also conducted. The time replicates were designated as Trial 1 and Trial 2. These data were statistically analyzed using SAS statistical software to determine the effects of the variables on shell thickness. For treatment effects, both sham-inoculated and vaccinated data were examined for age and treatment interactions.

One-day-old Single Comb White Leghorn pullets of a single genetic strain (Hy-Line variety W-36) were obtained from Hy-Line North America, LLC; Wilton, IA 52778, which were certified free of *Mycoplasma gallisepticum* (MG) and *Mycoplasma synoviae* (MS). At five weeks of age randomly sampled birds were tested to certify that they were free of MG infection. Pullets were maintained on clean dry litter to 12 weeks in a 5.5 m X 6.1 m section of

a conventional house at the United States Department of Agriculture, Agricultural Research Service (USDA-ARS)-Poultry Research Unit. Starter and grower diets were fed to pullets through 12 weeks of age as described by Burnham *et al.* (2002a). A daily artificial lighting schedule followed a 13 hours of light: 11 hours of dark schedule.

At 12 weeks of age, sham-inoculated (control) and FMG-inoculated birds were assigned to individual cages in one of two ends of the cage layer facility at the USDA-ARS-Poultry Research Unit. Birds were housed in the FMG-House consisting of a control end and an experimental end. A total of 480 birds were in Trial 1; 160 birds were included in Trial 2. Other than the number of birds in the two trials, the experimental methods were identical.

All birds were wing-banded for purposes of identification and individual data collection. Developer and pre-lay diets, which were provided between 12 and 20 weeks of age, were as described by Burnham *et al.* (2002a). Beginning at 18 weeks of age, the duration of the artificial lighting system was increased 15 minutes per day until a cycle of 16 hour 15 minute light and 7 hour 45 minutes dark was achieved. This artificial lighting program was maintained until the end of each Trial.

Three differently supplemented iso-caloric diets were administered to birds within each end of the layer house at 20 weeks of age, with all three dietary treatments assigned to birds belonging to each inoculation type (sham- or FMG-inoculated). Birds in each side of the house were watered, fed, and ventilated separately. Feed and water were provided for *ad libitum* consumption. The diets were as follows:

1. Normal basal control diet- basal control diet- contains 0.5% PF
2. Normal basal control diet plus 1.5% PF (2.0% PF total)
3. Normal basal control diet plus 1.5% PF (2.0% PF total) with supplemental phytase (0.013%) and 25-D3 (0.025%)

Two cages of birds were maintained for each set of variables (treatment and diet). Pullets treated with FMG were inoculated via eye drop in the right eye at 12 weeks of age with 0.04 mL of a 24-hour broth culture of high-passage FMG. Pullets designated as controls were sham-inoculated via eye drop in the right eye at 12 weeks of age with 0.04 mL of sterile Frey's broth medium.

Egg Collection Procedures and Shell Thickness Measurements

Egg collection was stratified so that there was equal representation of each of the independent variables, treatment group (sham-inoculated and FMG-inoculated) and diet. There were four replicates for each treatment-diet

combination, and eggs were collected at two time periods (24 and 50 weeks), resulting in the total collection of 48 eggs (Figure 1).

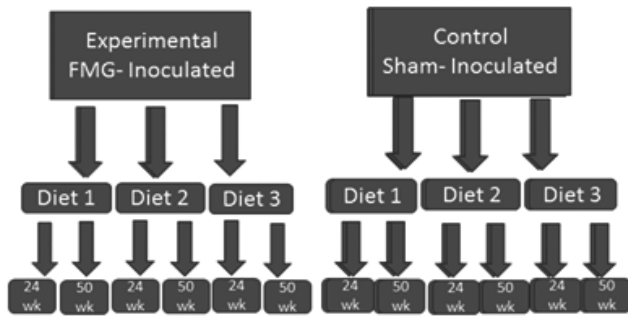


Figure 1. Experimental design for FMG trials. In both Trial 1 and Trial 2 birds were divided into two treatment groups, FMG-inoculated and sham-inoculated. Within each treatment group birds were subdivided into three diet groups, diet 1 (basal diet), diet 2 (normal basal diet plus 1.5% PF), and diet 3 (normal basal control diet plus 1.5% PF with supplemental phytase (0.013%) and 25-D3 (0.025%). Four eggs were collected from birds of each diet subgroup at 24 weeks and again at 50 weeks. A total of 48 eggs were collected for this experiment.

Eggs were numbered 1-48 and each egg was identified based on its variables using an Excel spreadsheet. The shell of each egg was broken and three samples were taken from the equator region (largest diameter) of each egg. The samples for each egg were mounted radially on separate aluminum pin stubs with for viewing the cross-section with the SEM. The stubs were sputter-coated with gold and palladium. Trial 1 samples were imaged using JOEL 35C SEM. Trial 2 samples were imaged using FEI Quanta 200, Mark II Environmental SEM. For each stub, each of the three samples was imaged with each cross section adjusted to present a flat surface to the microscope using the SEM rotation and tilt functions (Figure 2). A micrograph was made of each eggshell cross section at 200X magnification. The eggshell thickness was measured on cross section micrographs using Image Pro Plus software (Trial 1) and Image J software (Trial 2). Each micrograph was opened in the image analysis program. The scale was recalibrated using the image micron bar for each micrograph to ensure accuracy. Measurements of thickness of the shell were made by measuring the distance from the external edge of the outer shell surface (cuticle) to the tip of the mammillary cone at the internal shell surface. Three measurements were taken of each cross section in locations on the eggshell image that showed full view of the entire shell thickness. (Figure 3). Eggshell thickness data were accumulated in an excel document with identification of the variables for each sample: treatment, diet, and age of lay.

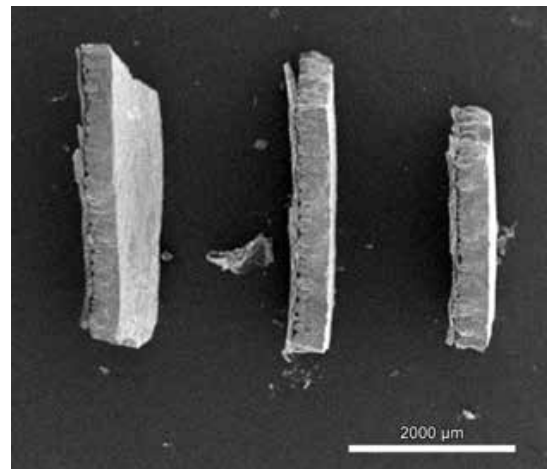


Figure 2. Montage of mounted eggshell cross sections for a single egg. Three cross section samples from the equator region of each of 48 eggs were mounted on stubs for SEM imaging (10X).

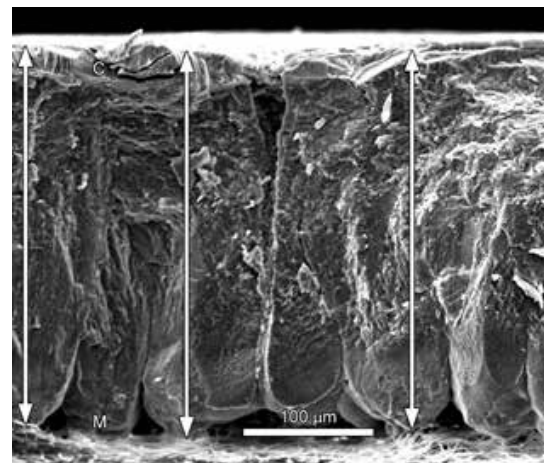


Figure 3. SEM of eggshell cross section with measurement arrows. The width of each eggshell cross section sample (white arrows) was measured at three locations from the external cuticle surface (C) to the tip of the mammillary cone (M) using image analysis software.

Statistical Analysis

A three-way factorial ANOVA with sub-sampling was used to analyze the effects of independent variables, treatment (control vs. inoculated), diet type (basal, basal plus phytase, and basal plus phytase and 25-D3), and age (24 weeks versus 50 weeks), on the dependent variable, eggshell thickness. According to the design of the experiment, each egg (represented by a single stub) was the experimental unit, and each measurement was the sampling unit. Thus, the experimental error was calculated at the egg (stub) level.

Results and Discussion

The means and standard error bars (at egg level) by treatment, diet, and age are presented in Figs. 4, 6, 8, and 10 (Trial 1) and Figs. 5, 7, 9, and 11 (Trial 2). There were

no significant main effects for treatment in either Trial 1 or Trial 2 (Figs. 8 and 9, respectively). There were also no significant main effects for age in either Trial 1 or Trial 2 (Figs. 10 and 11, respectively). There were no significant three-way interaction effects among treatment, diet and age for either Trial 1 (Fig. 4) or Trial 2 (Fig. 5). Treatment had no significant interaction effect with diet on eggshell thickness in either Trial 1 or 2 (Figs. 6 and 7, respectively). Treatment had no significant interaction effect with age of bird on eggshell thickness in either Trial 1 or 2 (Figs. 8 and 10, respectively). There were no significant effects from diet and age interactions in either Trial 1 or 2 (Figs. 10 and 11, respectively).

When comparing the mean values for all samples in Trial 1 ($374.38 \pm 24.61 \mu\text{m}$) with those of Trial 2 ($303.34 \pm 19.93 \mu\text{m}$) differences are apparent. Single Comb White Leghorn pullets of a single genetic strain (Hy-Line variety W-36) were used for both experiments. However, the birds for the two were obtained in different years, which may have resulted in genetic variation in the bird populations for the two trials. In addition, different SEM instruments were used in the two trials. Trial 1 samples were imaged using a JOEL 35C SEM, while Trial 2 samples were imaged using an FEI Quanta 200, Mark II Environmental SEM. Differences in the operating systems of the two instruments may have also resulted in systematic differences in the two trials. For example, the FEI Quanta 200 instrument is capable of more accurate working distance settings, which could affect the image and the relative eggshell thicknesses detected. Regardless of these differences between Trials 1 and 2, the findings were consistent for both trials with respect to the research hypotheses.

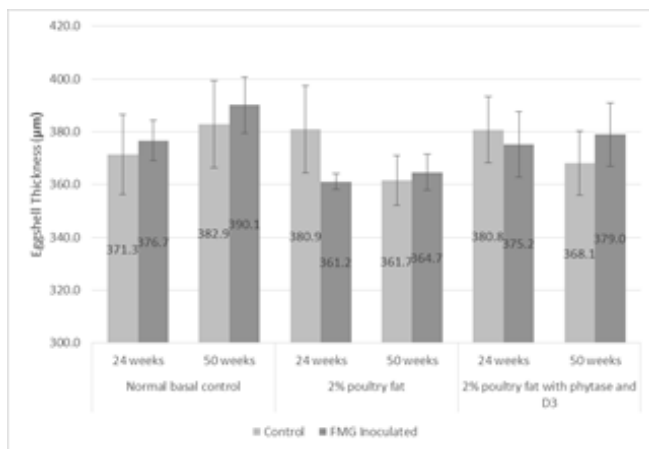


Fig. 4. Eggshell Thickness by Treatment, Diet, and Age (Trial 1). The three-way factorial ANOVA with subsampling showed that the three-way interaction effect among treatment, diet and age was not significant, $F(2, 36) = 0.203$, $p = .818$.

Other studies have also found that FMG inoculation does not affect eggshell characteristics. For example, Leigh *et al.* (2010) reported that FMG-inoculated birds did not exhibit a loss of eggshell strength. Also, in earlier studies by Branton *et al.* birds that were inoculated with FMG via eye drops were reported to have no change in eggshell strength patterns (Branton *et al.* 1988, Branton *et al.* 1997). Additional studies by Peebles, *et al.* (2003, 2008) have investigated the effect of diet supplements in the form of 1.5% PF, phytase, and 25-D3 on FMG-inoculated birds. Peebles *et al.* (2003) concluded that dietary supplementation did not affect egg production or eggshell characteristics of the eggs produced by FMG-inoculated birds.

In contrast to our findings, however, others have found FMG inoculation to affect the birds' reproductive physiology. For example, Burnham *et al.* (2002b) reported that inoculation with FMG resulted in changes in birds' reproductive organs including ovarian follicular regression and reduced reproductive tract length. Also, Burnham *et al.* (2002a) found that birds inoculated with FMG exhibited a delayed initiation of lay and lower weekly egg production. In the same study, Burnham *et al.* (2002a) also found that eggshell weights (calculated as percent shell weight of entire egg weight) in FMG-inoculated birds were found to be significantly higher compared to those of control birds, regardless of the age of lay, 24 or 36 weeks. They concluded that this may mean that FMG-inoculated birds deposited relatively more calcium carbonate on eggs during peak production than those not inoculated with FMG. In addition, Park *et al.* (2010) stated that inoculation with FMG may change the oviduct by altering the contribution of the mass of the isthmus and infundibulum.

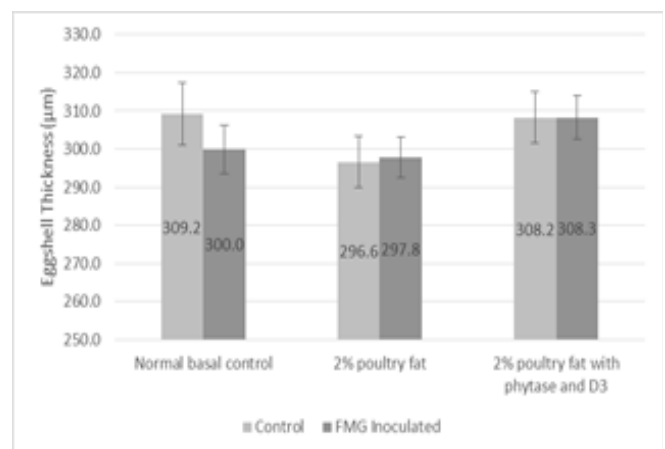


Fig. 5. Eggshell Thickness by Treatment, Diet, and Age (Trial 2). The three-way factorial ANOVA with subsampling showed that the three-way interaction effect among treatment, diet and age was not significant, $F(2, 36) = 1.965$, $p = .155$.

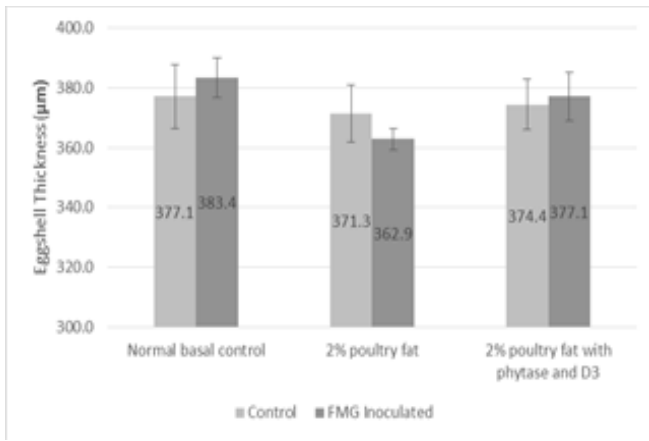


Fig. 6. Eggshell Thickness by Treatment and Diet (Trial 1). The three-way factorial ANOVA with sub-sampling showed that the two-way interaction effect between treatment and diet was not significant, $F(2, 36) = 0.416$, $p = .663$.

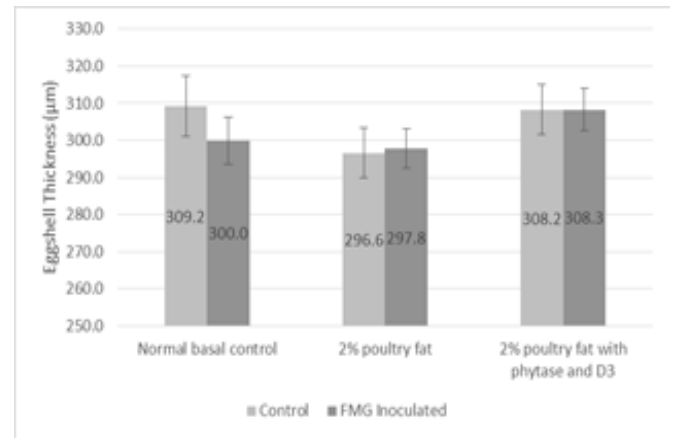


Fig. 7. Eggshell Thickness by Treatment and Diet (Trial 2). The three-way factorial ANOVA with sub-sampling showed that the two-way interaction effect between treatment and diet was not significant, $F(2, 36) = 0.373$, $p = .692$.

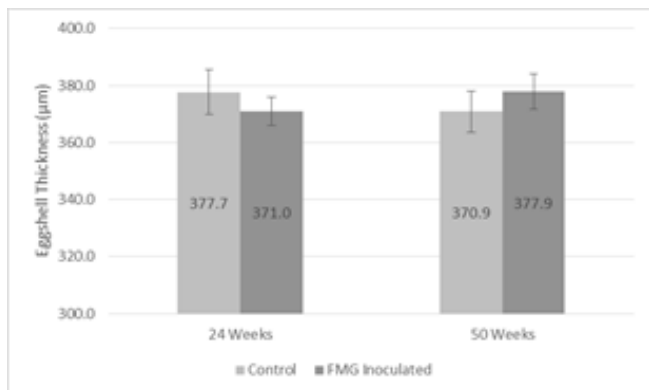


Fig. 8. Eggshell Thickness by Treatment and Age (Trial 1). The three-way factorial ANOVA with sub-sampling showed that the two-way interaction effect between treatment and age was not significant, $F(1, 36) = 0.994$, $p = .325$. The main effect of treatment was not significant, $F(1, 36) = .001$, $p = .977$.

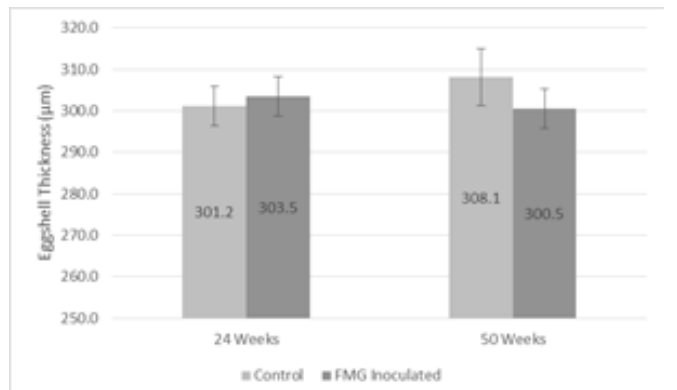


Fig. 9. Eggshell Thickness by Treatment and Age (Trial 2). The three-way factorial ANOVA with sub-sampling showed that the two-way interaction effect between treatment and age was not significant, $F(1, 36) = .838$, $p = .366$. The main effect of treatment was not significant, $F(1, 36) = .243$, $p = .625$.

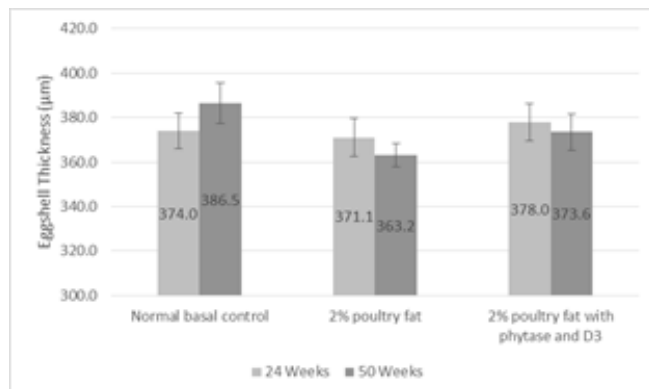


Fig. 10. Eggshell Thickness by Diet and Age (Trial 1). The three-way factorial ANOVA with sub-sampling showed that the two-way interaction effect between diet and age was not significant, $F(2, 36) = 0.843$, $p = .439$. The main effect of diet was not significant, $F(2, 36) = 1.266$, $p = .294$. The main effect of age was not significant, $F(1, 36) = .000$, $p = .993$.

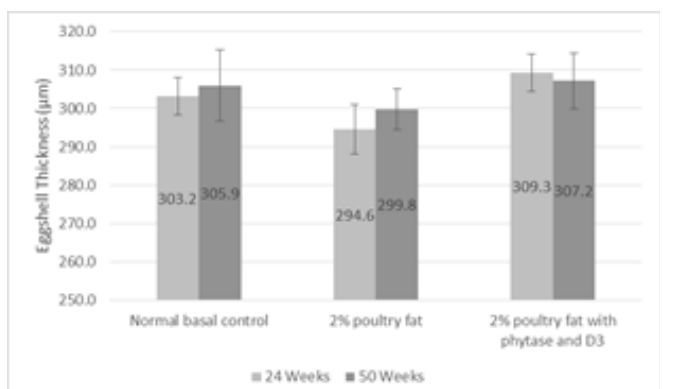


Fig. 11. Eggshell Thickness by Diet and Age (Trial 2). The three-way factorial ANOVA with sub-sampling showed that the two-way interaction effect between diet and age was not significant, $F(2, 36) = .161$, $p = .852$. The main effect of diet was not significant, $F(2, 36) = 1.455$, $p = .247$. The main effect of age was not significant, $F(1, 36) = .135$, $p = .716$.

We conclude from the current study that FMG inoculation does not affect shell thickness, regardless of age of lay (24 or 50 weeks) or diet (basal control or enhancement with PF, and phytase with 25-D3). Although the factors in this investigation, including inoculation with FMG, age of bird at lay, and diet, may affect the reproductive tract in some ways, our study shows that these effects may not become manifest in the thickness of the shells that were examined.

This study provides an innovative method for the use of electron microscopy and image analysis for examination of shell thickness. Future studies using this eggshell analysis method could be conducted to relate eggshell thicknesses or other microstructural eggshell characteristics to length of reproductive tract, date of initiation of lay, weekly egg production, and percent shell weight for FMG-inoculated and control birds.

Acknowledgements

The authors express appreciation to Weidan Zhou, John Maddoux, and Dr. Doyle Hawkins for their help with statistical analysis. This project was funded by USDA-ARS research grant SCA#58-6406-4-102 to E. David Peebles.

References

- Branton, S. L., B. D. Lott, J.W. Deaton, J. M. Hardin, and W. R. Maslin. 1988. F strain *Mycoplasma gallisepticum* vaccination of post-production-peak commercial Leghorns and its effect on egg and eggshell quality. *Avian Dis.* 32:304-307.
- Branton, S.L., B. D. Lott, J. D. May, W. R. Maslin, C. R. Boyle, and G. T. Pharr. 1997. The effects of F-strain *Mycoplasma gallisepticum*, *Mycoplasma synoviae*, and the dual infection in commercial layer chickens of a 44-week laying cycle when challenged before beginning of lay. I. Egg production and selected egg quality parameters. *Avian Dis.* 41:832-837.
- Burnham, M. R., S. L. Branton, E. D. Peebles, B. D. Lott, P. D. Gerard. 2002. Effects of F-strain *Mycoplasma gallisepticum* inoculation at twelve weeks of age on performance and egg characteristics of commercial egg laying hens. *Poult. Sci.* 81:1478-1485.
- Burnham, M. R., E. D. Peebles, S. L. Branton, M. S. Jones, P. D. Gerard, W. R. Maslin. 2002. Effects of F-strain *Mycoplasma gallisepticum* inoculation at twelve weeks of age on digestive and reproductive organ characteristics of commercial egg laying hens. *Poult. Sci.* 81:1884-1891.
- Burnham, M. R., E. D. Peebles, S. L. Branton, D. V. Maurice, P. D. Gerard. 2003. Effects of F-strain *Mycoplasma gallisepticum* inoculation at twelve weeks of age on egg yolk composition in commercial egg laying hens. *Poult. Sci.* 82:577-584.
- Khan, M. I., D. A. McMartin, R. Yammoto, and H. B. Ortmyer. 1986. Observations on commercial layers vaccinated with *Mycoplasma gallisepticum* (MG) bacteria on multiple-age site endemically infected with MG. *Avian Dis.* 30:309-312.
- Leigh, S.A., S. L. Branton, J. D. Evans, S. D. Collier, and E. D. Peebles. 2010. Effects on vaccination with F-strain *Mycoplasma gallisepticum* on egg production and quality parameters of commercial layer hens previously vaccinated with 6/85-strain *Mycoplasma gallisepticum*. *Poult. Sci.* 89:501-504.
- Park, S.W., M. R. Burnham, S. L. Branton, P. D. Gerard, S. K. Womack, and E. D. Peebles. 2010. Influence of supplemental dietary poultry fat on the digestive and reproductive organ characteristics of commercial layers inoculated before or at the onset of lay with F-strain *Mycoplasma gallisepticum*. *Poult. Sci.* 89:248-253.
- Peebles, E. D., S. L. Branton, M. R. Burnham, and P. D. Gerard. 2003. Influences of supplemental dietary poultry fat and F-strain *Mycoplasma gallisepticum* infection on the early performance of commercial egg laying hens. *Poult. Sci.* 82:596-602.
- Peebles, E. D., S. L. Branton, M. R. Burnham, S. K. Whitmarsh, and P. D. Gerard. 2008. Effects of supplemental dietary phytase and 25-hydroxcholecalciferol on the performance characteristics of commercial layers inoculated before or at the onset of lay with the F-strain of *Mycoplasma gallisepticum*. *Poult. Sci.* 87:598-601.
- Vance, A.M., S. L. Branton, S. D. Collier, P. D. Gerard, and E. D. Peebles. 2009. Effects of time-specific F-strain *Mycoplasma gallisepticum* inoculation overlays on prelay ts-1-strain *M. gallisepticum* vaccination on digestive and reproductive organ characteristics of commercial egg-laying hens. *Poult. Sci.* 88:980-983.



Multi Application CPD Autosamdri®-931

Mouse Rachea processed by Autosamdri®-931 / SEM Image courtesy Pat Kysar (C.E.M.T., SRA III) EM Lab, UC Davis.

tousimis® CPD Benefits

- *Advanced Manual to Fully Automatic*
- *Free Lifetime Tech Support*
- *2 Year Warranty*
- *Made in U.S.A.*

Autosamdri®-931 Features

- ✓ Patent Pending "Stasis Software" for Challenging Sample
- ✓ Multi Application Touch Screen Critical Point Dryer
- ✓ Fully Automatic & Custom Programmable Recipes
- ✓ Available in Three Chamber Sizes
- ✓ Cleanroom System Option

Corporate Members



AMETEK (EDAX), Inc.

Tina Wolodkowicz
392 East 12300 South, Suite H
Draper, UT 84020
(801) 4952872
www.ametek.com

BioTek Instruments

Vanessa Meyer
100 Tigan St. | Winooski, VT 05404
(888) 451-5171
customercare@biotek.com
www.biotek.com

Boeckeler Instruments/RMC Products

Dave Roberts
4650 S. Butterfield Dr. | Tucson, AZ 85714
(520) 745-0001
dave@boeckeler.com

CARL ZEISS SMT

German Neal
One Corporation Way | Peabody, MA 01960
(978) 826-1500 | FAX (978) 532-5696
neal@smt.zeiss.com
www.zeiss.com/nts

Bruker AXS, Inc.

John Mastovich
5465 East Cheryl Parkway
Madison, WI 53711-5373
(800) 234-XRAY

E. A. FISCHIONE INSTRUMENTS

Nicole M. Dengler
9003 Corporate Circle | Export, PA 15632
(724) 325-5444, x261
nm_dengler@fischione.com

EDAX, Inc.

John Haritos
91 Mckee Dr. | Mahwah, NJ 07430
(201) 466-0907
John.Haritos@ametec.com

Electron Microscopy Sciences/Diatome

Rob Armstrong
P.O. Box 550
1560 Industry Rd. | Hatfield, PA 19440
(800)-523-5874 | (215) 412-8400
Fax (215) 412-8450
rarmstrong@emsdiasum.com
www.emsdiatome.com

FEI Company

James Ranney
5350 NE Dawson Creek Drive
Hillsboro, OR 97124
(503) 724-3038
james.ranney@fei.com
www.fei.com

Gatan, Inc.

James Long
5794 W. Las Positas Blvd.
Pleasanton, CA 94588
(512) 657-0898
info@gatan.com
www.gatan.com

Hitachi High Technologies America

Rod Baird
1375 N 28th Ave, P.O. Box 612208
Dallas, TX 75218
(214) 537-2158
rod.baird@hitachi-hta.com
www.hitachi-hta.com

IXRF Systems

3019 Alvin DeVane Blvd, Suite 130
Austin, TX 78741
(512) 386-6100 | FAX (512) 386-6105
www.ixrfsystems.com

JEOL USA, Inc.

Zane Marek
District Sales Manager
13810 Paisano Circle | Austin, TX 78737
(978) 495-2176
marek@jeol.com
www.jeol.com

Leica Microsystems, Inc.

Drew Roberston
1700 Leider Lane
Buffalo Grove, IL 60089
(713) 823-5366 | FAX 847-607-7024
www.microsystems.com

McBain Systems

Leica Industrial Microscopes
2665 Park Center Dr. Bldg. A
Simi Valley, CA 93065
(805) 581-5200
www.mcbainsystems.com

MicroStar Technologies, Inc.

Cathy Ryan
511 FM 3179 | Huntsville, TX 77340
(936) 291-6891
cathy.ryan@microstartech.com
www.microstartech.com

Nikon Instruments, Inc.

Michael Johnson
1300 Walt Whitman Road
Melville, NY 11747
(800) 52-NIKON Office
(214) 738-0210 | FAX (631) 547-8652
mjohnson@nikon.net
www.nikoninstruments.com

Park Systems: Atomic Force Microscopy

Frank Coppertino
3040 Olcott Street
Santa Clara, CA 95054
(408) 986-1110
frank.coppertino@gmail.com
www.parkafm.com

Ted Pella, Inc.

4595 Mountain Lakes Blvd.
Redding, CA 96003
(800) 237-3526 | FAX (530) 243-2200
sales@tedpella.com
www.tedpella.com

TESCAN USA Inc.

Mike Craig, Heather Holdaway
and Colleen Leary
765 Commonwealth Drive, Suite 101
Warrendale, PA 15086
(724) 772-7433
accounting@tescan-usa.com
holdaway@tescan-usa.com
cleary@tescan-usa.com
www.tescan-usa.com

Thermo Fisher Scientific

Thomas O'Connor
81 Wyman St. | Waltham, MA 02451
(800) 766-7000
thomas.oconnor@thermofisher.com
www.thermo.com/microanalysis

Tousimis Research Corporation

Hyun Park
2211 Lewis Ave.
Rockville, MD 20851-2333
(310) 881-2450 | FAX (301) 881-5374
trc@tousimis.com
www.tousimis.com

VISIT TSM WEBSITE

Visit us at [http:// www.texasmicroscopy.org](http://www.texasmicroscopy.org) to take a look at important features such as membership, meetings, journal issues, small grant program and more!



The screenshot shows the homepage of the Texas Society for Microscopy (TSM). The header features the TSM logo (a map of Texas with 'TSM' and 'e' in a circle) and the text 'TEXAS SOCIETY FOR MICROSCOPY' and the tagline 'Embracing All Forms of Microscopy'. A navigation menu includes links for HOME, ABOUT US, MEMBERSHIP, MEETINGS, JOURNALS, SMALL GRANT, and LINKS. The main content area is divided into three columns. The left column, titled '** Next TSM Meeting **', lists the dates 'February 19 - 21, 2015' at the 'Holiday Inn Austin Town Lake', with the address '20 North IH-35, Austin, TX 78701'. It includes a link to the 'Program on Meetings page' and a 'MAP' button. Below this is a Facebook 'Join us on facebook' button with the text 'TSM is on Facebook!'. The middle column, titled 'TSM Annual Meeting', describes the 50th anniversary meeting held from February 19-21, 2015, at the Holiday Inn Austin Town Lake. It mentions a workshop on Thursday, February 19, and provides a link to 'download the Meeting Program'. The right column, titled 'MEETINGS OF INTEREST', features the logo for 'M&M 2015 MICROSCOPY & MICROANALYSIS' and states that the meeting will be held from August 2-6, 2015, in Portland, OR, with a link to 'Learn more...'. The background of the website features a large, detailed micrograph of a biological specimen, possibly a beetle or insect, showing its intricate structure.

JOIN TEXAS SOCIETY FOR MICROSCOPY ON FACEBOOK



The screenshot shows the Facebook page for the Texas Society for Microscopy. The profile picture is the TSM logo. The cover photo shows an older man and a woman looking at a scientific poster titled 'TEXAS WORKSHOP: A SCANNING ELECTRON MICROSCOPY ANALYSIS BETWEEN STRUCTURE AND FUNCTION OF SCALES IN HEAVY METAL EXPOSED WESTMOOREL'. The page header includes the text 'Texas Society for Microscopy Non-Profit Organization' and buttons for 'Like', 'Follow', and 'Message'. The navigation menu shows 'Timeline', 'About', 'Photos', 'Likes', and 'More'. The main content area shows a post from the 'Texas Society for Microscopy' page, dated March 9, 2015, which states: 'Texas Society for Microscopy added 117 new photos to the album: 50th Meeting of the Texas Society for Microscopy 2015 — at UT Austin.' Below the post, there is a link to the website: 'http://www.texasmicroscopy.org/index.html'. The page also shows '58 people like this' and an 'Invite friends to like this Page' button.

IN MEMORIAM DR. ELIZABETH ANN ELLIS

It is with sadness that we announce the passing away of Dr. Elizabeth Ann Ellis, long-time member of the Texas Society for Microscopy, on October 29 2016. Ann earned a Bachelor's degree from the University of Georgia, a Master's degree from the University of North Carolina at Chapel Hill, and a Doctorate from the University of Florida. While studying for her Ph.D., she performed research in ophthalmology and endocrinology. Dr. Ellis taught electron microscopy techniques, and as a senior research associate at the Texas A&M Microscopy and Imaging Center worked with faculty and other microscopists on diverse research projects for 10 years before retiring in 2013. She had an impressive record of scholarship with more than 100 publications in scientific journals. As a member of the Texas Society of Microscopy, Southeastern Microscopy Society and Microscopy Society of America, Ann received numerous awards as distinguished electron microscopist and outstanding technologist and was the co-editor of the Texas Journal of Microscopy from 2010-2012. Ann will be missed by all who were fortunate to get to know her.



Ann with Sandra Westmoreland
at a coffee break at 2012 TSM meeting



Attending the registration table
at the 2010 TSM meeting

CALL FOR PAPERS

Authors are invited to submit their manuscripts for the next edition of the Texas Journal of Microscopy. The objective of the journal is to publish papers on original research and developing methods for providing prospect guidelines to research supported by all forms of microscopy. Please send your work as short communications, full articles or review articles in biological sciences, material sciences or education to either journal editor:

Camelia Maier
cmaier@twu.edu

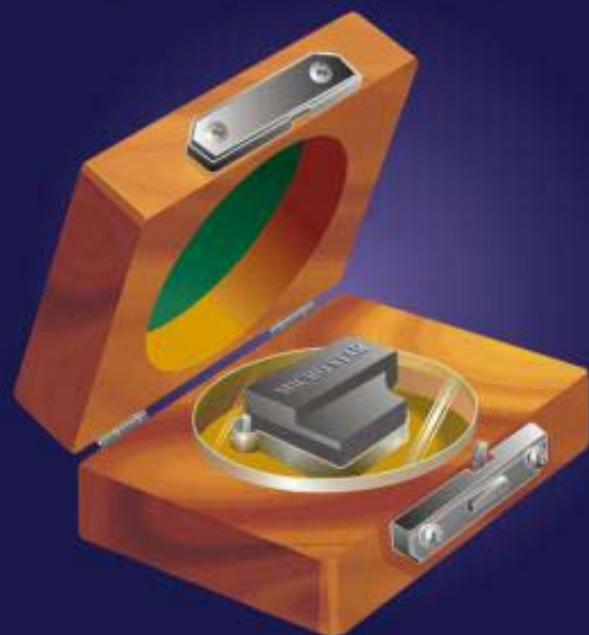
Nabarun Ghosh
nghosh@mail.wtamu.edu

MICRO STAR DIAMOND KNIFE

TYPES

TYPES	AVAILABLE EDGE LENGTHS	AVAILABLE INCL. ANGLES*	RANGE OF SECTION THICKNESS	APPLICATIONS
SU	1 to 8 mm	45° 35° 55°	25nm to 200nm	Standard ultramicrotomy sectioning of biological and other material specimens.
CW	1 to 8 mm	45° 35°	50nm to 1 μ m	Frozen specimens sectioned wet with liquids like ethylene glycol. Set in "W" style boat.
CD	1 to 8 mm	45° 35°	50nm to 1 μ m	Frozen specimens sectioned dry. Set in "D" style boat.
TS	1 to 8 mm	45° 55°	50nm to 2 μ m	Thick sections or alternating thick and thin sections.
MT	2 to 8 mm	45° 55°	50nm to 2 μ m	Industrial materials sectioning. Not tested to the same ultra high standards as the types above, hence their lower price.
LC	4 to 12 mm	45° 55°	0.1 μ m to 5 μ m	Frozen specimens to be examined at light microscopy magnifications. Set in "D" or "W" style boat.
LH	4 to 12 mm	45° 55°	0.1 μ m to 5 μ m	Sections to be examined at light microscopy magnifications.

* The standard included angle of 45° is suitable for most applications. Knives with 35° reduce morphological deformation but the edge is more fragile. 55° is recommended for routine hard specimen sectioning. Custom angles and lengths available per request at no extra cost.



MICRO STAR diamond knives are manufactured exclusively from the purest quality natural diamonds, using the most advanced technologies. Our quality inspection laboratory includes two TEM one SEM and one Atomic Force Microscope.

MICRO STAR is the only diamond knife whose unsurpassed quality is backed by one year guarantee, and two month testing period before payment.

Every MICRO STAR diamond knife is packaged in a precision hand crafted wood case for life time shipping and storage protection.

Per request, you may get your resharpened knife set in a new MICRO STAR boat and box at no extra cost.

MICRO STAR TECHNOLOGIES
511 FM 3179 RD
HUNTSVILLE, TX 77340
936-291-6891

EMS has it!

A comprehensive selection of the finest hand-made tweezers for every research requirement, including...

- Medical Tweezers
- High Precisions and Ultra Fine Tweezers
- Thin and Long
- Ergonomic
- Flat Tip
- Ceramic and Ceramic Tipped
- ESD Safe
- General Purpose Tweezers
- Fiber and Fiber Tipped
- EMS Synthetic Fiber Tweezers
- Surface Mount and Optoelectric
- Wafer

and our newest additions:

EMS Gold Coated Tweezers

Finely crafted, high precision tweezers made from anti-acidic, non-magnetic stainless steel, plated with 2 microns of pure 24-carat gold.



EMS High Precision, Diamond Like Carbon (DLC) Tweezers

Feature tips covered in a pure diamond film grown directly on the exposed metallic substrate via an innovative plasma-assisted deposition technique.



now also available
in medical grade...

EMS Tweezers

NEW EMS High End Medical Tweezers

EMS is proud to introduce this new category of tweezers. They are all handcrafted to perfect tip symmetry and balance and the surface has an electropolish finish. With high precision fine tips and dot-serrated handles for a perfect grip. All of these tweezers can be sterilized and they are all made from Inox.



EMS is proud to provide a full selection of tweezers and forceps with all hand-crafted to a perfect tip symmetry and balance, high quality and innovative tweezers, that are well suited for many applications:

EM Labs • General Labs • Electronic • Aerospace • Precision Assembly • Optics • Biotech • Chemistry • Surgery • and more

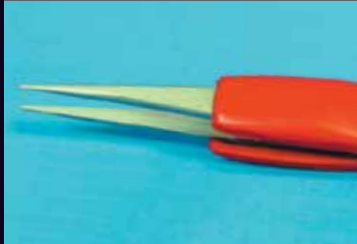
CONTACT US FOR
MORE INFORMATION...

**Electron
Microscopy
Sciences**

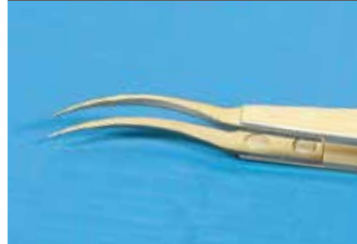
P.O. Box 550 • 1560 Industry Rd.
Hatfield, Pa 19440
Tel: (215) 412-8400
Fax: (215) 412-8450
email: sgkcck@aol.com
or stacie@ems-secure.com

www.emsdiasum.com

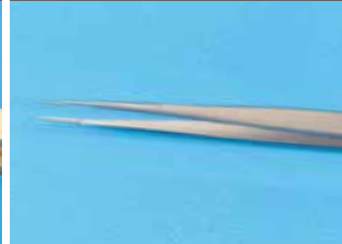
ESD SAFE
TWEEZERS



ERGONOMIC
TWEEZERS



SUPER SLIM
TWEEZERS



FLAT TIP
TWEEZERS



CERAMIC TIP
TWEEZERS



WAFER
TWEEZERS

